Systematic Analysis of the Lysine Malonylome in *Sanghuangporus Sanghuang*

Tong Wang
Shandong Province Key Laboratory of Applied Mycology, Qingdao Agricultural University
Guangyuan Wang
Shandong Province Key Laboratory of Applied Mycology, Qingdao Agricultural University
Guoli Zhang
Shandong Province Key Laboratory of Applied Mycology, Qingdao Agricultural University
Ranran Hou
Shandong Province Key Laboratory of Applied Mycology, Qingdao Agricultural University
Liwei Zhou
State Key Laboratory of Mycology, Institute of Microbiology, Chinese Academy of Sciences
Xuemei Tian (txm@qau.edu.cn)
Shandong Province Key Laboratory of Applied Mycology, Qingdao Agricultural University

Research Article

Keywords: Malonylation, Post-translational modification (PTM), Malonylproteome, Sanghuangporus sanghuang

Posted Date: December 18th, 2020

DOI: https://doi.org/10.21203/rs.3.rs-128142/v1

Version of Record: A version of this preprint was published at BMC Genomics on November 19th, 2021.
See the published version at https://doi.org/10.1186/s12864-021-08120-0.

Abstract

Background: *Sanghuangporus sanghuang* is a well-known traditional medicinal mushroom associated with mulberry, which has enormous economic and medical value. Despite being known for many years, proteomics studies of *S. sanghuang* have not been reported. In this paper, a series of technologies, such as high-performance liquid chromatography (HPLC) classification technology, malonyl peptide segment enrichment technology and proteomics technology, are combined to study the qualitative analysis of malonylation in *S. sanghuang.*

Results: Strategies for qualitative proteomics included malonyl enrichment and high-resolution liquid chromatography-tandem mass spectrometry (LC-MS/MS). In total, 714 malonyl modification sites were matched to 255 different proteins. The analysis indicated that malonyl modifications are involved in a wide range of acellular functions and displayed a distinct subcellular localization.

Bioinformatics analysis indicates that malonylated proteins are engaged in different metabolic pathways, including glyoxylate and dicarboxylate metabolism, glycolysis/gluconeogenesis, and the tricarboxylic acid (TCA) cycle; consequently, a total of 26 enzymes related to triterpene and polysaccharide biosynthesis were found to be malonylated.

Conclusions: These findings suggest that malonylation is associated with many metabolic pathways, particularly the metabolism of bioactive compounds. This paper provides the first comprehensive survey of malonylation in *S. sanghuang.*

Background

Sanghuangporus sanghuang (Sheng H. Wu, L.W. Zhou & Y.C.) Sheng H. Wu, L.W. Zhou & Y.C. Dai belongs to Basidiomycota, Hymenochaetales, Hymenochaetaceae and *Sanghuangporus* and has been used for more than 2000 years in China. It has been previously mistaken for *Inonotus linteus* or *Inonotus baumii* for a long time, was identified as a new species, *Inonotus sanghuang*, in 2012 and was renamed *S. sanghuang* in 2016 [1, 2].

Extensive work has shown that *S. sanghuang* has a diverse range of biological activities, such as anti-diabetic, antitumor, antibacterial, anti-inflammatory and anti-radiation activities [3–6]. The active substances that play a major role in this medicinal fungus of *S. sanghuang* are triterpenoids and polysaccharides. Consequently, the demand for consumption urges *S. sanghuang* to be a highly promising fungus for industrial development. In recent years, proteomic data have been widely used to elucidate the mechanisms of biologically active compounds [7]. Currently, the regulation of biosynthesis of *S. sanghuang* bioactive compounds is still unclear.

Post-translational modifications (PTMs) serve a pivotal part in modulating different cellular pathways and disease processes, and over 400 distinct forms of PTMs have been found [8]. Lysine malonylation is an evolutionarily conserved PTM. Lysine malonylation is enriched in metabolic pathways, especially

glycolysis and the synthesis of bioactive substances. Malonylation has been reported to use malonyl-CoA as a substrate in the reaction [9]. At present, with advances in high-throughput experimental techniques, thousands of peptide segments containing lysine malonylation have been discovered. These data have strengthened the basic understanding of the sequence and structural features of lysine malonylation in chloroplasts [10], the mitochondria [11], the cytoplasm [7, 12], and the nucleus [13, 14], as well as in the discovery of lysine malonylation, suggesting that lysine malonylation is regulated in a diverse manner.

Lysine malonylation is reported to be a functional PTM that affects bacterial metabolism and metabolic enzyme activity [15], but few studies have examined the mushroom malonyl proteome. Hence, we conducted a qualitative proteomics study of malonylated proteins in *S. sanghuang*. We postulated that lysine malonylation may affect various metabolic processes in *S. sanghuang*. To demonstrate this hypothesis, we performed a functional analysis of all malonylated proteins, and the results provided a comprehensive view of the regulation of lysine malonylation in a wide range of biological processes, notably in the biosynthesis of bioactive metabolites and secondary metabolites.

Methods

Fungal strain

The *S. sanghuang* mycelia used in this study were isolated from fruit bodies collected from the mountainous area of Anshun city, Guizhou Province, China. The specimen was deposited in the Mycological Herbarium, Qingdao Agricultural University (HMQAU), Qingdao. Morphological and molecular identification of the *S. sanghuang* strain was performed according to a previous study [16–18].

Protein extraction and trypsin digestion

Grind the tissue samples to powder in a pre-cooled mortar with liquid nitrogen. A four-fold volume of phenol extraction buffer containing 10 mM dithiothreitol, 1% protease inhibitor, 3 μM trichostatin A, and 50 mM nicotinamide was added and lysed by sonication. Equivalent volumes of Tris equilibrium phenol were added, and samples were centrifuged at 5500 × g and 4 °C for 10 min. Supernatants were collected and sedimented overnight with a 5-fold volume of 0.1 M ammonium acetate, and the protein precipitate was washed with methanol and acetone. Then, 8 M urea was re-dissolved for precipitation. Finally, measuring protein concentration using bicinchoninic acid (BCA) kits.

Then, 20% trichloroacetic acid was slowly added to the protein solution, and the sample was vortexed and precipitated at temperature of 4 °C for 2 h. After centrifugation at 4500 × g for 5 min, the supernatant was discarded, and the precipitate was washed 2–3 times with precooled acetone. After drying the precipitate, 200 mM tetraethylammonium bromide (TEAB) was added, and the mixture was sonicated to break up the precipitate. Trypsin was then added to enzymatically digest the sample overnight. At 56 °C, 5 mM dithiothreitol was added to the sample and incubated for 30 min; then, 11 mM iodoacetamide was added and incubated for 15 min at room temperature without light.

HPLC fractionation and affinity enrichment

High-pH reverse HPLC fractionation was used for peptides on an Agilent 300 Extend C18 column (5 μm, 4.6 mm, 250 mm). The operation was performed as follows: sterilized peptide fractions were isolated in a gradient between 8%-32% acetonitrile (pH = 9) for 60 min. They were merged into 4 fractions and freeze-dried under vacuum.

The polypeptides were dissolved in IP buffer (100 mM NaCl, 1 mM ethylenediaminetetraacetic acid (EDTA), 50 mM Tris-HCl, and 0.5% NP-40 (pH 8.0)), and the superfluid was transferred to malonylated resin (PTM-904, PTM Biolabs, Hangzhou Jingjie Biotech Co., Ltd.). The resin was gently shaken and incubated on a rotating shaker at 4 °C overnight. Following incubation, the resin was cleaned four times with IP buffer and twice with deionized water. Finally, the resin was eluted three times with 0.1% trifluoroacetic acid eluent, and the eluent was collected and freeze-dried. Desalting was performed in accordance with the C18 ZipTips [19–21] instructions and freeze-dried under vacuum for HPLC analysis.

LC-MS/MS analysis

Dissolved the peptide with solvent A (0.1% formic acid) and separated by ultrahigh-performance liquid chromatography (UHPLC) using EASY-nLC 1000. Mobile phase A consisted of 0.1% formic acid and 2% acetonitrile. Mobile phase B consisted of 0.1% formic acid and 90% acetonitrile. The liquid phase gradient was set as follows: 0–20 min, 7%-25% B; 20–34 min, 25%-38% B; 34–37 min, 38%-80% B; and 37–40 min, 80% B, with a flow rate of 500 nL/min.

After HPLC separation, the peptides were injected into a nanospray ionization (NSI) ion source for ionization and mass spectrometry (MS) analysis. The ion source voltage was set to 2.2 kV. The primary MS scanning range was 350–1800 m/z, and the secondary MS scanning range was 100.0 m/z. Data collection was performed using the data-dependent acquisition (DDA) procedure. The automatic gain control (AGC) was set to 5e4. [22], The dynamic rejection time was set to 15 s to avoid repeated scanning, the parameter threshold was set to 5e3 ions/s, and the maximum injection time was set to 200 ms.

Database search

Secondary MS data were analysed with MaxQuant [23]. The search parameters were set as follows: the database was *S. sanghuang* (transcriptome, 23290 sequences). Reverse libraries were added to reduce false positives, and contamination libraries were added to eliminate the effects of contaminated proteins. The enzymatic method applied was Trypsin/P. The missed cut bin count was set to 4. The first search and main search primary parent ion mass error tolerance was set to 20 ppm and 5 ppm, respectively. Cysteine alkylation was set as the fixed modification, and the variable modifications were the acetylation of the protein N-terminus, deamidation of aspartylation/glutamylation, and malonylation of lysine. All false discovery rates (FDRs) of these were set to 1% [24].

Bioinformatics analyses

Gene Ontology (GO) annotations of proteins are classified mainly among three categories: biological process, cellular component, and molecular function [25]. GO annotations of the proteomics results were

from the UniProt-Gene Ontology Annotation (GOA) database [26]. InterProScan [27] predicts GO functions of proteins that are not in the database for the queried proteins, classifying them by their cellular composition, cellular function or specific metabolic processes [28]. Annotated the protein pathway using the Kyoto Encyclopedia of Genes and Genomes (KEGG) database. Involvement of the submitted proteins in subcellular localization was annotated using WoLF PSORT [29]. Fisher's exact (two-sided) test was used for the identification of modified proteins on the basis of the corresponding proteins of the species, and the p value was required to be less than 0.05. The GO enrichment test p value was deemed significant for values that were less than 0.05 [30–32]. Abundance analysis of KEGG pathways and analysis of protein domains with a p value < 0.05 were deemed significant. [33, 34].

The differentially modified protein database numbers from the different comparison groups were compared with those from the Search Tool for the Retrieval of Interacting Genes/Proteins (STRING) [35] protein-protein interaction (PPI) network database based on confidence scores greater than 0.7. Then, the visualization of the differential PPI network was presented with the R package "networkD3" [36, 37].

Results

Proteome-scale analysis of malonylated proteins in S. sanghuang

In this project, a range of technologies, such as HPLC, malonylation peptide enrichment and MS-based proteomics technologies, were combined to study the qualitative proteomics of malonylation in *S. sanghuang* (Fig. 1a). The results showed that the peptide score was between − 10 and 10 (Fig. 1b). The tolerance of peptides was in a reasonable range. The distribution of identified peptide lengths was examined, and the lengths of most peptides were between 7 and 22 (Fig. 1c), meeting the requirements of proteomic analysis. The MS results of malonylated peptides are summarized in Additional file 1: Fig. S1. Consequently, 713 malonyl-modified sites matched to 255 different proteins were identified in *S. sanghuang* (Additional file 2: Table S1). Among them, many are related to triterpene synthesis. Farnesyl pyrophosphate synthases (FPPs), which are are pivotal enzymes in the main pathway of triterpene synthesis, the mevalonate (MVA) pathway, were found to be malonylated.

Pattern analysis of malonylated sites

For the purpose of valuing the distribution of malonylation sites in *S. sanghuang*, the number of identified modification sites was calculated for each protein. As shown in Fig. 2a, 47% of the proteins had one malonylation site, while only 18%, 7%, 12%, 3%, and 13% of the proteins contained 2, 3, 4, 5, and 6 or more modification sites, respectively. It has been documented that modification positions are prioritized at specific sites for lysine (Additional file 2: Table S3). Therefore, the compositional frequencies of the amino acids surrounding lysine were examined. In Fig. 2c, lysine (K) had the highest frequencies in the − 10 to + 10 position, whereas arginine (R) and glutamate (E) had the lowest frequencies. Hence, proteins with this group are the preferred substrates for malonyltransferases in *S. sanghuang.* Consistent with the

results of the motif enrichment heatmap (Fig. 2b), only one motif was detected. K indicates modified lysine sites and * denotes random amino acid sites (Fig. 2d). To elucidate the secondary structure of proteins and the correlation between modified lysines, the secondary structures of all malonylated proteins in *S. sanghuang* were examined (Fig. 2e). The malonylation sites are located more in the coiled-coil regions (P = 0.18) than in the α-helical (P = 0.01) and β-strand (P = 0.48) regions, suggesting that malonylation may favour the disordered structures of *S. sanghuang.* In addition, we assessed the surface accessibility on lysine malonylated sites and found 39.62% of the unmodified lysine residues were located on the protein surface, compared to 39.54% of the modified lysine sites (Fig. 2f). As such, the protein's surface accessibility may be influenced by lysine malonylation.

Functional annotation and cellular localization of malonylated proteins in S. sanghuang

To obtain a better comprehension of the malonylated proteins in *S. sanghuang.* Upon their corresponding biological processes and molecular functions, we annotated and classified the identified proteins. GO analysis showed that malonylated proteins had extensive activity molecular functions and biological processes in *S. sanghuang*. The group of malonylated proteins in the largest classification of biological processes consists of enzymes related to metabolism (53%) (Fig. 3a). The majority of malonylated proteins were associated with organocyclic compound binding (15%), heterocyclic compound binding (15%) and structural constituent of ribosome (10%) within the molecular functional classification (Fig. 3b). Characterization of the subcellular localization of malonylated proteins showed the modified proteins were found in the cytoplasm (36%), mitochondria (31%), and nucleus (21%) (Fig. 3c). Consequently, malonylated proteins have multiple functions and are broadly found in *S. sanghuang.*

Functional enrichment analysis of malonylated proteins

To summarize and analyse the proteins and their functions, we performed functional enrichment analysis of the obtained malonylome by GO and KEGG pathway and protein domains analyses (Additional file 2: Table S5, Additional file 2: Table S6). Proteins associated with structural components of the ribosome were highly enriched by functional analysis of GO molecules (Additional file 2: Table S4). Based on GO cellular component classification, proteins that are located in the ribosomal subunit, ribosome, large ribosomal subunit, small ribosomal subunit, and cytosol are more likely to be malonylated (Additional file 1: Fig. S2). The domain enrichment studies indicated that these proteins are core histone H2A/H2B/H3/H4, proteasome, beta-ketoacyl synthase, 1-cys peroxiredoxin, acyl transferase domain, isocitrate/isopropyl malate dehydrogenase, and oxidoreductase flavin adenine dinucleotide (FAD) binding domain (Additional file 1: Fig. S3). These enriched domains play a crucial role in glycolysis, polysaccharide synthesis and the tricarboxylic acid (TCA) cycle in *S. sanghuang*. Thus, malonylated proteins participate in a myriad of cellular processes. To probe the process of malonylation regulation, we performed enrichment analysis of proteins corresponding to malonylation modification sites in KEGG pathways (Fig. 4). Several pathways of the enriched proteins in the ribosome, glucuronide and

dicarboxylic acid metabolism, TCA cycle, glycolysis/gluconeogenesis and pyruvate metabolism were shown. Conclusively, malonylated proteins are enriched in several types of proteins and pathways and play a pivotal role in the lysine malonylation of *S. sanghuang*..

PPI network of malonylated proteins in S. sanghuang

To determine how the identified proteins are associated with multiple pathways, a PPI network was constructed. Ninety proteins were detected in the PPI database. (Fig. 5, Additional file 2: Table S7), presenting a global vision of how the identified malonyl proteins are involved in the multiple pathways of *S. sanghuang*. Analysis of the STRING PPI network with Cytoscape identified three heavily correlated clusters of malonylated proteins, including those associated with ribosomes, metabolic pathways, and biosynthesis of secondary metabolites in *S. sanghuang*. Above all, we conclude that malonylation is a critical PTM for proteins in *S. sanghuang* and helps interactions and coordination with diverse pathways.

Malonylated proteins associated with the biosynthesis of bioactive compounds in S. sanghuang

Malonylated proteins were identified based on functional enrichment, and proteins related to ribosomes, glucuronide and dicarboxylic acid metabolism, glycolysis/gluconeogenesis, TCA cycle, methane metabolism, oxidative phosphorylation, and pyruvate metabolism were found to be greatly enriched (Fig. 4). These findings suggested that the malonylation of lysine may be essential in the biosynthesis of bioactive compounds in *S. sanghuang.* To further confirm these findings, we analysed malonylated proteins associated with triterpene and polysaccharide biosynthesis in *S. sanghuang*. Consistent with these hypotheses, the TCA cycle, glycolysis supplied compounds for the biosynthesis of triterpenoids and polysaccharides. A grand total of 26 enzymes associated with triterpene and polysaccharide biosynthesis were found to be malonylated (Fig. 6, Additional file 2: Table S8). In Fig. 6, a large number of enzymes are supported by malonylation in glycolysis and TCA cycle, suggesting that malonylation may be associated with multiple levels of intracellular metabolism. Furthermore, our results also showed that 51 malonyl modified sites detected on ribosomes, such as ribosomal proteins L24, L13a, and S3, were closely tied up bioactive functions (Fig. 7).

Discussion

In this paper, we performed the first proteomic survey of lysine malonylation in *S. sanghuang*. It has been reported that *S. sanghuang* is capable of producing many active substances, such as terpenes, flavonoids, and polysaccharides [38–41]. The metabolic processes of bioactive substances are related to secondary metabolism. Our malonyl analysis revealed a great number of malonylated proteins participating in secondary metabolism, demonstrating the essential character of lysine malonylation in all these processes. Acetylation, succinylation and other types of PTMs also participate in secondary

metabolic processes in fungi [7, 14]. The identified malonylated proteins participate in a diverse range of bioprocesses and are notably abundant in metabolic processes. As shown in Fig. 6, malonylation uses malonyl-CoA as a substrate in the reaction. The source of malonyl-CoA is the carboxylation of acetyl-CoA. The key enzyme catalysing the carboxylation reaction is acyl-CoA carboxylases (ACCs). ACCs play pivotal roles in primary and secondary metabolism. The first enzyme in the (MVA) pathway is acetyl-CoA acetyltransferase (ACAT), which converts acetyl-CoA to acetoacetyl-CoA. FPPs are crucial enzymes in the MVA pathway of triterpene metabolism [42]. Further modification of terpenes involves the introduction of acyl, aryl, or glycosyl groups, usually starting with oxidation catalysed by cytochrome P450 monooxygenases (P450s, also known as CYPs). P450s are ubiquitous in nature and are involved in fundamental biological pathways such as terpene biosynthesis [43–46]. All these key enzymes were detected by malonyl-enriched modifications. Thus, lysine malonylation plays a multilevel regulatory role in the biosynthesis of secondary metabolism enzymes. As shown in Fig. 7, different types of ribosomal proteins may have different biological activities. Ribosomal protein S5 (RPS5) is closely associated with liver fibrosis [47]. RPS13a plays a role in plant defence against *Verticillium dahliae* infection [48]. RPS3 has antioxidant activity [49]. RPL24 is associated with anticancer activity [50]. In addition, ribosomal synthesis and post-translationally modified peptides (RiPPs) are an important family of bioactive products [51]. These findings all support the irreplaceable role of protein malonylation in the synthesis of bioactive substances.

Conclusions

Proteomic analysis of *S. sanghuang* by lysine malonylation fills a gap in the knowledge of Chinese medicinal fungi. It was reported that *S. sanghuang* is responsible for the production of many active substances, such as terpenoids, flavonoids and polysaccharides. The malonylated proteins identified are involved in a variety of biological processes, especially in secondary metabolic pathways. First time malonyl modification sites on ribosomes were found in *S. sanghuang* for possible different bioactivities. These discoveries also led to the emergence of *S. sanghuang* as a functional food and medical health product with promising applications.

Declarations

Acknowledgements

Not applicable

Authors’ contributions

TW conceived and designed the study and drafted the manuscript. GW participated in the design and discussion of the research and helped to carefully revise English editing.GZ participated in the design and provided technical implementation assistance. RH participated in the design and provided technical

implementation assistance. LZ participated in the discussion of the research and revised English editing. XT participated in its design and coordination and exercised general supervision. All authors read and approved the final manuscript.

Funding

The research was supported by the National Natural Science Foundation of China (Project No. 31772376, 31970014, 31301827); University Youth Innovation and Technology Program of Shandong Province, China (Project No. 2019KJE003); Research Foundation of Qingdao Agricultural University, China (Project No. 631445)

Availability of data and material

All data generated or analysed during this study are included in this published article and its supplementary information files.

Ethics approval and consent to participate

Not applicable.

Consent for publication

Not applicable.

Competing interests

The authors declare that they have no competing interests.

Author details

1 Shandong Province Key Laboratory of Applied Mycology, Qingdao Agricultural University, Changcheng Road, No.700, Qingdao 266109, China.

2State Key Laboratory of Mycology, Institute of Microbiology, Chinese Academy of Sciences, Beijing 100101, China

References

1. Zhou LW, Ghobad-Nejhad M, Tian XM, Wang YF, Wu F. Current Status of '*Sanghuang*' as a Group of Medicinal Mushrooms and Their Perspective in Industry Development. Food Reviews International. 2020;DOI:10.1080/87559129.2020.1740245.
2. Tian XM, Dai YC, Song AR, Xu K, Ng LT. Optimization of Liquid Fermentation Medium for Production of *Inonotus sanghuang*(Higher Basidiomycetes) Mycelia and Evaluation of their Mycochemical Contents and Antioxidant Activities. International Journal of Medicinal Mushrooms. 2015;17(7):681-691.
3. Cheng J, Song J, Liu Y, Lu N, Wang Y, Hu C, He L, Wei H, Lv G, et al. Conformational properties and biological activities of α-D-mannan from *Sanghuang porus sanghuang* in liquid culture. International journal of biological macromolecules. 2020;164:3568-3579..
4. Lin W, Deng J, Huang S, Wu S, Chen C, Lin W, Lin H, Huang G. Anti-Inflammatory Activity of *Sanghuangporus sanghuang* Mycelium. International Journal of Molecular Sciences. 2017;18(2):347.
5. Ma X, She X, Peterson EC, Wang YZ, Zheng P, Ma H, Zhang K, Liang J. A newly characterized exopolysaccharide from *Sanghuangporus sanghuang*. Journal of Microbiology. 2019;57(9):812-820.
6. Sun Y, Zhong S, Yu J, Zhu J, Ji D, Hu G, Wu C, Li Y. The aqueous extract of Phellinus igniarius (SH) ameliorates dextran sodium sulfate-induced colitis in C57BL/6 mice. Plos One. 2018;13(10):1-13.
7. Zhou S, Yang Q, Yin C, Liu L, Liang W. Systematic analysis of the lysine acetylome in Fusarium graminearum. BMC genomics. 2016;17(1):1019.
8. Ma YY, Yang MK, Lin XH, Liu X , Huang H, Ge F. Malonylome Analysis Reveals the Involvement of Lysine Malonylation in Metabolism and Photosynthesis in Cyanobacteria (Article). Journal of Proteome Research. 2017;16(5):2030-2043.
9. Zhou BD, Du YP, Xue YJ, Miao GB, Wei TB, Zhang P. Identification of Malonylation, Succinylation, and Glutarylation in Serum Proteins of Acute Myocardial Infarction Patients. Proteomics Clinical Applications. 2020;14(1):1-6.
10. Liu J, Wang G, Lin Q, Liang W, Gao Z, Mu P, Li G, Song L. Systematic analysis of the lysine malonylome in common wheat. BMC Genomics. 2018;19(1):209.
11. Bowman CE, Wolfgang MJ. Role of the malonyl-CoA synthetase ACSF3 in mitochondrial metabolism. Advances In Biological Regulation. 2019;71:34-40.
12. Bowman CE, Rodriguez S, Alpergin ESS, Acoba MG, Zhao L, Hartung T, Claypool SM, Watkins PA, Wolfgang MJ. The Mammalian Malonyl-CoA Synthetase ACSF3 Is Required for Mitochondrial Protein Malonylation and Metabolic Efficiency. Cell chemical biology. 2017;24(6):673-684e4.
13. Sophie T, Claudia DL, Nathaniel WS, Kathryn EW. Compartmentalised acyl-CoA metabolism and roles in chromatin regulation. Molecular metabolism.2019;38:100941.

14. Guang YW, Xu LL, Yu H, Gao J, Guo LZ. Systematic analysis of the lysine succinylome in the model medicinal mushroom Ganoderma lucidum. BMC Genomics. 2019;20(1):585.
15. Fan B, Li Y, Li L. Malonylome analysis of rhizobacterium Bacillus amyloliquefaciens FZB42 reveals involvement of lysine malonylation in polyketide synthesis and plant-bacteria interactions(Article). Journal of Proteomics. 2017;154:1-12.
16. Chang HY, Shih SY, Yu TW, Wu SH, Hattori T, Parmasto E, Wang DM, Dai YC: Species clarification for the medicinally valuable '*sanghuang*' mushroom. Botanical Studies. 2012;53(1):135-149.
17. Tian XM, Yu HY, Zhou LW, Decock C, Vlasak J, Dai YC: Phylogeny and taxonomy of the *Inonotus linteus* complex(Article). Fungal Diversity.2013;58(1):159-169.
18. Zhou LW, Vlasak J, Decock C: Global diversity and taxonomy of the *Inonotus linteus* complex (Hymenochaetales, Basidiomycota): *Sanghuangporus* gen. nov., Tropicoporus excentrodendri and *T guanacastensis* gen. et spp. nov., and 17 new combinations. Fungal Diversity.2016;77(1):335-347.
19. Schmelter C, Funke S, Treml J. Comparison of Two Solid-Phase Extraction (SPE) Methods for the Identification and Quantification of Porcine Retinal Protein Markers by LC-MS/MS. Advanced Techniques in Biology & Medicine. 2018;6(3):9.
20. Schmelter C, Funke S, Treml J, Beschnitt A, Perumal N, Manicam C, Pfeiffer N, Grus FH. Comparison of Two Solid-Phase Extraction (SPE) Methods for the Identification and Quantification of Porcine Retinal Protein Markers by LC-MS/MS. International Journal of Molecular Sciences. 2018;19(12):3847.
21. Yang Z, Shen X, Chen D, Sun L. Microscale Reversed-Phase Liquid Chromatography/ Capillary Zone Electrophoresis-Tandem Mass Spectrometry for Deep and Highly Sensitive Bottom-Up Proteomics: Identification of 7500 Proteins with Five Micrograms of an MCF7 Proteome Digest(Article). Analytical Chemistry. 2018;90(17): 10479-10486.
22. Ameli A, Hooshyar A, Yazdavar AH, El-Saadany EF, Youssef A. Attack detection for load frequency control systems using stochastic unknown input estimators. IEEE Transactions on Information Forensics and Security. 2018;13(10):2575-2590.
23. Tyanova S, Temu T, Cox J. The MaxQuant computational platform for mass spectrometry-based shotgun proteomics(Article). Nature Protocols. 2016;11(12):2301-2319.
24. An Z, Zhai L, Ying W, Qian X, Gong F. PTMiner. Localization and Quality Control of Protein Modifications Detected in an Open Search and Its Application to Comprehensive Post-translational Modification Characterization in Human Proteome. Molecular & cellular proteomics. 2019;18(2):391-405.
25. Wang R, Wang C, Sun L, Liu G. A seed-extended algorithm for detecting protein complexes based on density and modularity with topological structure and GO annotations. BMC Genomics. 2019;20(1):1-28.
26. Wei X, Zhang C, Freddolino PL, Zhang Y. Detecting Gene Ontology Misannotations Using Taxon-Specific Rate Ratio Comparisons. Bioinformatics (Oxford, England). 2020;10: btaa548.

27. Shah A, Joseph, Schielzeth H. Transcriptome assembly for a colour-polymorphic grasshopper (Gomphocerus sibiricus) with a very large genome size. BMC Genomics 2019;20(1):1-10..
28. Jiao X, Sherman BT, Huang DW, Stephens R, Baseler MW, Lane HC, Lempicki RA. DAVID-WS: A stateful web service to facilitate gene/protein list analysis(Article). Bioinformatics. 2012;28(13):1805-1806.
29. Kanehisa M, Sato Y. KEGG Mapper for inferring cellular functions from protein sequences. Protein Science. 2020;29(1):28-35.
30. Mengozzi M, Hesketh A, Bucca G, Ghezzi P, Smith CP. Vitamins D3 and D2 have marked but different global effects on gene expression in a rat oligodendrocyte precursor cell line(Article). Molecular Medicine. 2020;26(1):1-11.
31. Gao Y, Li SP, Lai ZY, Zhou ZH, Wu F, Huang YZ, Lan XY, Lei CZ, Chen H, Dang RH. Analysis of Long Non-Coding RNA and mRNA Expression Profiling in Immature and Mature Bovine (Bos taurus) Testes. Frontiers In Genetics. 2019;10:646.
32. Wang Y, Wu CY, Zhang F, Zhang YN, Ren ZW, Guo X. Screening for Differentially Expressed Circular RNAs in the Cartilage of Osteoarthritis Patients for Their Diagnostic Value. Genetic Testing And Molecular Biomarkers. 2019;23(10):706-716.
33. Lotfan M, Ali SA, Yadav ML, Choudhary S, Jena MK, Kumar S, Mohanty AK.Genome-widegene expression analysis of 45 days pregnant fetal cotyledons vis-a-vis non- pregnant caruncles in buffalo (Bubalus bubalis). Gene. 2018;654:127-137.
34. Yan M, Jing X, Liu Y, Cui X. Screening and identification of key biomarkers in bladder carcinoma. Evidence from bioinformatics analysis. Oncology Letters.2018;16(3):3092-3100.
35. Szklarczyk D, Morris JH, Cook H, Kuhn M, Wyder S, Simonovic M, Santos A, Doncheva NT, Roth A, Bork P, et al. The STRING database in 2017: Quality-controlled protein-protein association networks, made broadly accessible(Article). Nucleic Acids Research. 2017;45 (D1):D362-D368.
36. Qi JP, Rui Z, Min S, Rong L. The Effects of Plumbagin on Pancreatic Cancer: A Mechanistic Network Pharmacology Approach. Medical sciencemonitor: international medical journal of experimental and clinical research. 2019;25:4648-4654.
37. Sween D, Vandana S, Pawan K, Ajit K. Protein-Protein interaction network analyses of human WNT proteins involved in neural development. Bioinformation. 2019;15(5): 307-314.
38. Ge Q, Mao JW, Zhang AQ, Wang YJ, Sun Pl. Purification, chemical characterization, and antioxidant activity of a polysaccharide from the fruiting bodies of *sanghuang* mushroom (Phellinus baumii Pilát). Food Science and Biotechnology. 2013;22(2):301-307.
39. Ma XK, She X, Peterson EC, Wang YZ, Zheng P, Ma H, Zhang K, Liang J. A newly characterized exopolysaccharide from *Sanghuangporus sanghuang*. Journal of Microbiology. 2019;57(9):812-820.
40. Ran L, Zou Y, Cheng J, Lu F. Silver nanoparticles in situ synthesized by polysaccharids from *Sanghuangporus sanghuang* and composites with chitosan to prepare scaffolds for the regeneration

of infected full-thickness skin defects. International journal of biological macromolecules. 2019;125:392-403.

41. Wen Y, Wan YZ, Qiao CX, Xu XF, Wang J, Shen Y. Immunoregenerative effects of the bionically cultured *Sanghuang*mushrooms (*Inonotus sanghuagn*) on the immunodeficient mice. Journal of Ethnopharmacology. 2019;245:1-9
42. Qi Q, Li R, Gai Y, Jiang XN. Cloning and functional identification of farnesyl diphosphate synthase from Pinus massoniana Lamb(Article). Journal of Plant Biochemistry and Biotechnology. 2017;26(2):132-140.
43. Mnguni FC, Padayachee T, Chen W, Gront D, Yu JH, Nelson DR, Syed K. More P450s Are Involved in Secondary Metabolite Biosynthesis in Streptomyces Compared to Bacillus, Cyanobacteria, and Mycobacterium. International journal of molecular sciences. 2020; 21(13):e4814.
44. Karunanithi PS, Berrios DI, Wang S, Davis J, Shen T, Fiehn O, Maloof JN, Zerbe P. The foxtail millet (Setaria italica) terpene synthase gene family. The Plant Journal. 2020;103(2):781-800.
45. Lemire CA, Mafu S. Elucidation of Terpenoid Biosynthesis in Sclerotinia. The FASEB Journal. 2020;34(Suppl 1):1.
46. Rudolf JD, Chang CY. Terpene synthases in disguise: enzymology, structure, and opportunities of non-canonical terpene synthases. Natural Product Reports. 2020;37(3):425-463.
47. Xu WH, Hu HG, Tian Y. Bioactive compound reveals a novel function for ribosomal protein S5 in hepatic stellate cell activation and hepatic fibrosis. Hepatology (Baltimore, Md). 2014;60(2):648-660.
48. Yang L, Xie C, Li W, Zhang R, Jue D, Yang Q. Expression of a wild eggplant ribosomal protein L13a in potato enhances resistance to Verticillium dahliae. Plant Cell, Tissue and Organ Culture. 2013;115(3):329-340.
49. Ahn EH, Kim DW, Shin MJ, Kim YN, Kim HR, Woo SJ, Kim SM, Kim DS, Kim J, Park J,et al: PEP-1-ribosomal protein S3 protects dopaminergic neurons in MPTP-induced Parkinson's disease mouse model. Free radical biology & medicine. 2012;55:36-45
50. Hou YL, Ding X, Hou W. Overexpression, purification, and pharmacologic evaluation of anticancer activity of ribosomal protein L24 from the giant panda (Ailuropoda melanoleuca). Genetics and Molecular Research. 2013;12(4):4735-4750.
51. Cao L, Gurevich A, Alexander KL, Naman CB, Leão T, Glukhov E, Luzzatto-Knaan T, Vargas F, Quinn R, Bouslimani A,et al. MetaMiner: A Scalable Peptidogenomics Approach for Discovery of Ribosomal Peptide Natural Products with Blind Modifications from Microbial Communities. Cell systems. 2019;9(6):600-608e604.

Figures

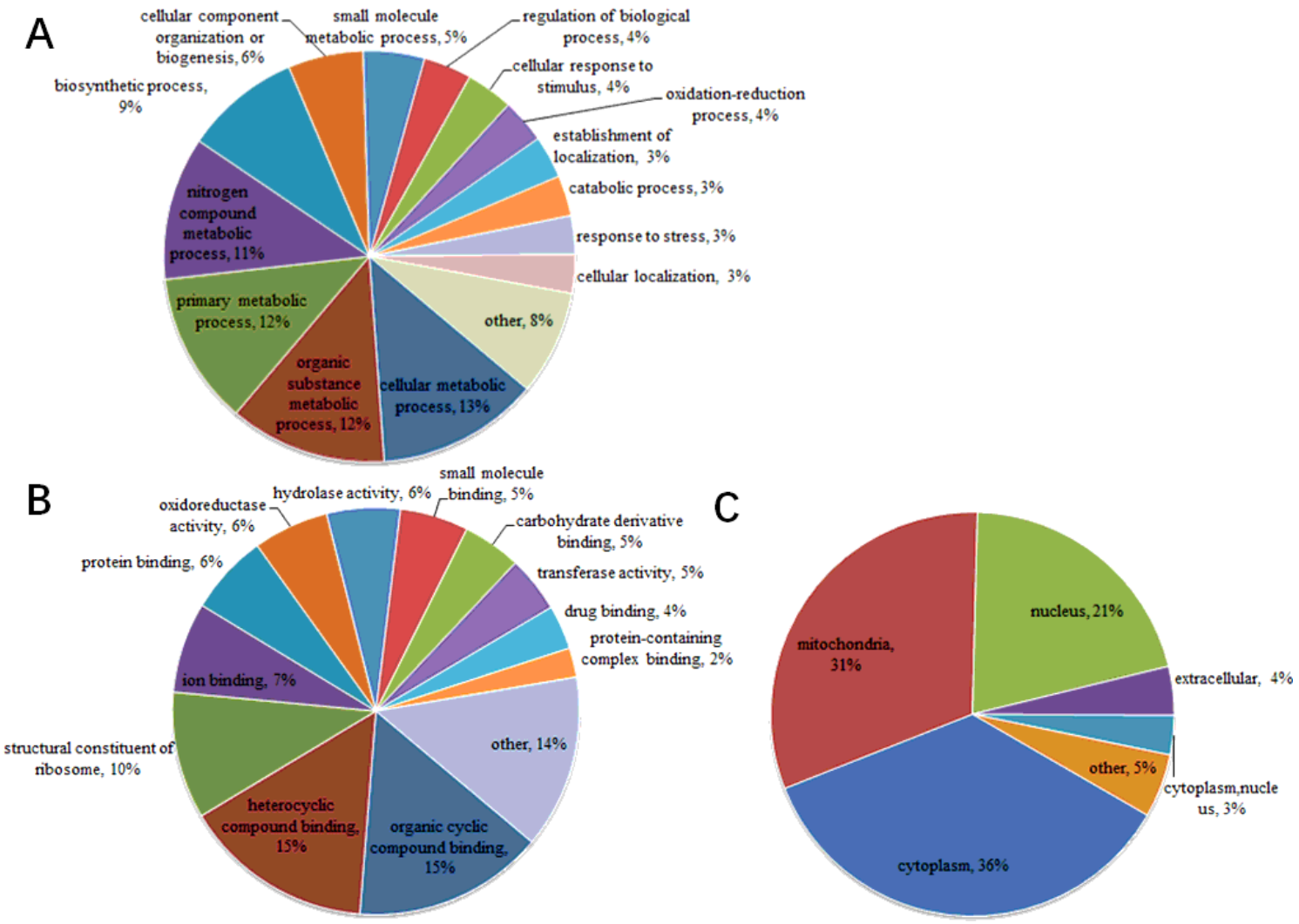

Figure 1

Functional classification of malonylated proteins in S. sanghuang. a Classify malonylated proteins based on biological process. b Classify malonylated proteins based on molecular function. c Subcellular localization of the malonylated proteins. The GO annotation classifies proteins according to their biological processes and molecular functions. A pie chart showing the percentage of malonylated proteins in each category.

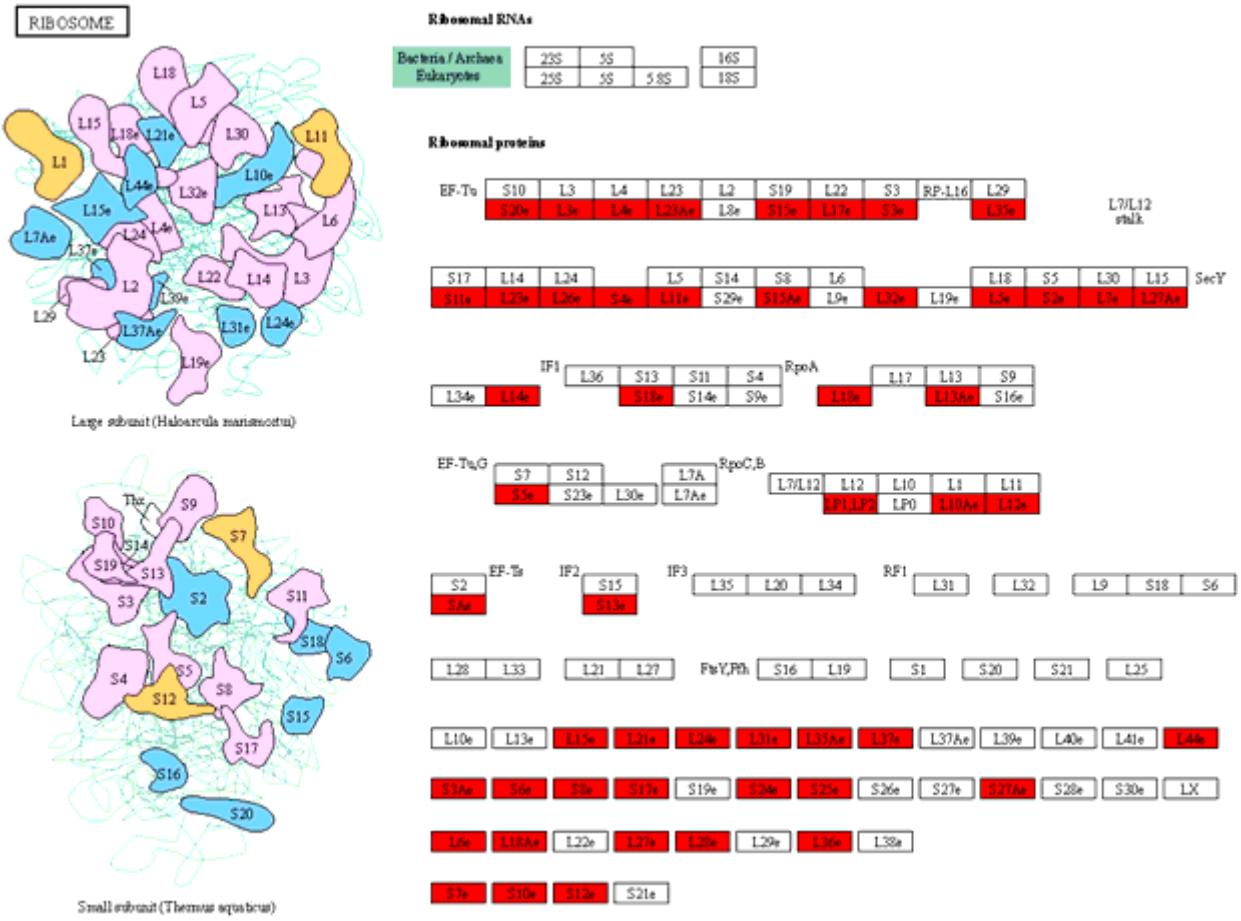

Figure 1

Malonylated modified sites on ribosomal proteins in S. sanghuang. The malonylated modified sites were highlighted in red.

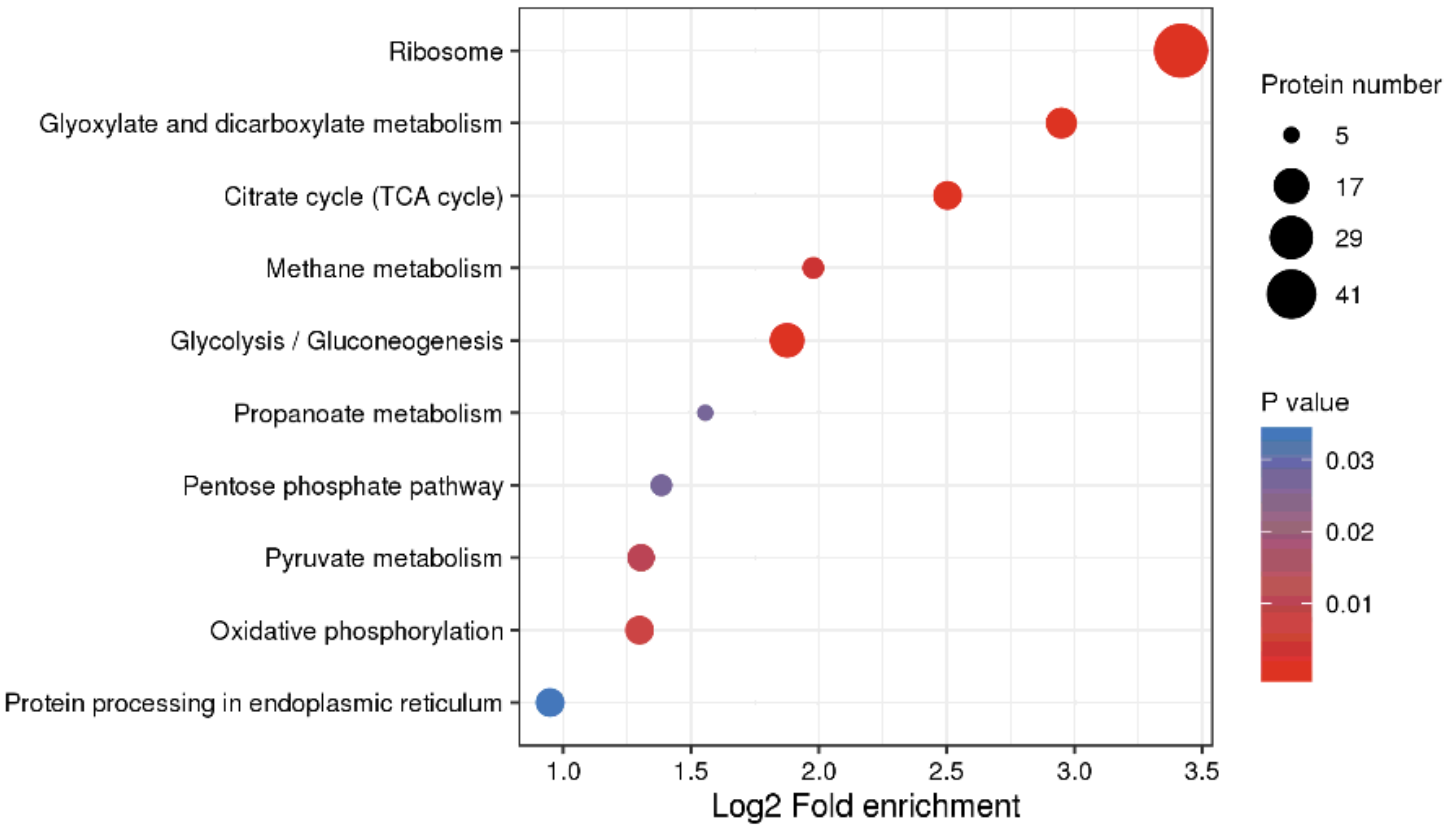

Figure 1

KEGG pathway enrichment bubble plot of proteins corresponding to modification sites in S. sanghuang

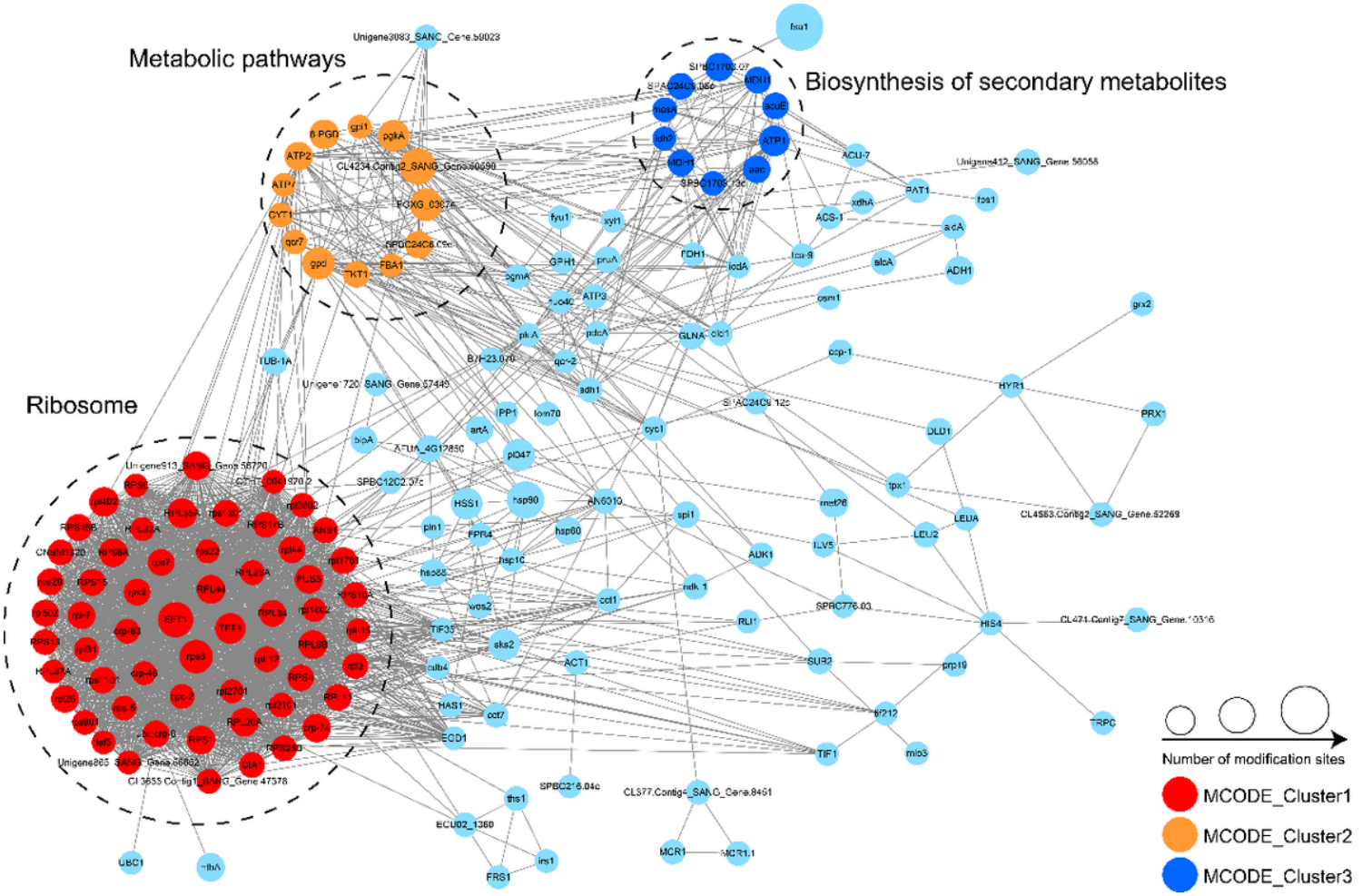

Figure 1

PPI network of malonylated proteins in S. sanghuang

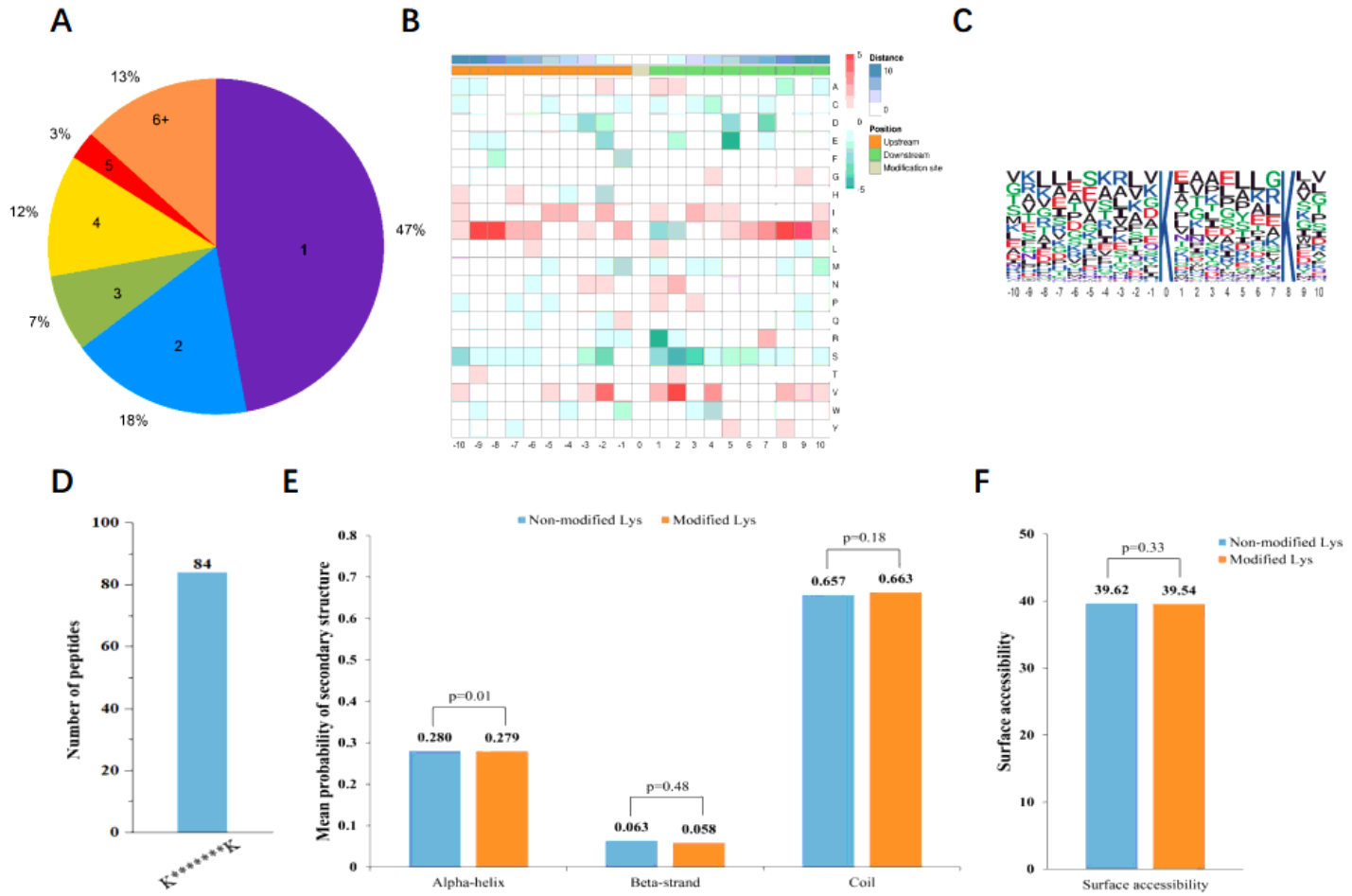

Figure 1

Characterization of malonylation sites. a Pie chart of the percentage and number of malonylated residues in the protein. b The frequency heat map of amino acid composition around malonylation c Conservatism of malonylation sites. Each letter's size pairs with the frequency of the amino acid at that site.. d Number of malonylation motif peptides. e Secondary structure analysis of malonyl protein. f Peptides surface accessibility of malonylation sites

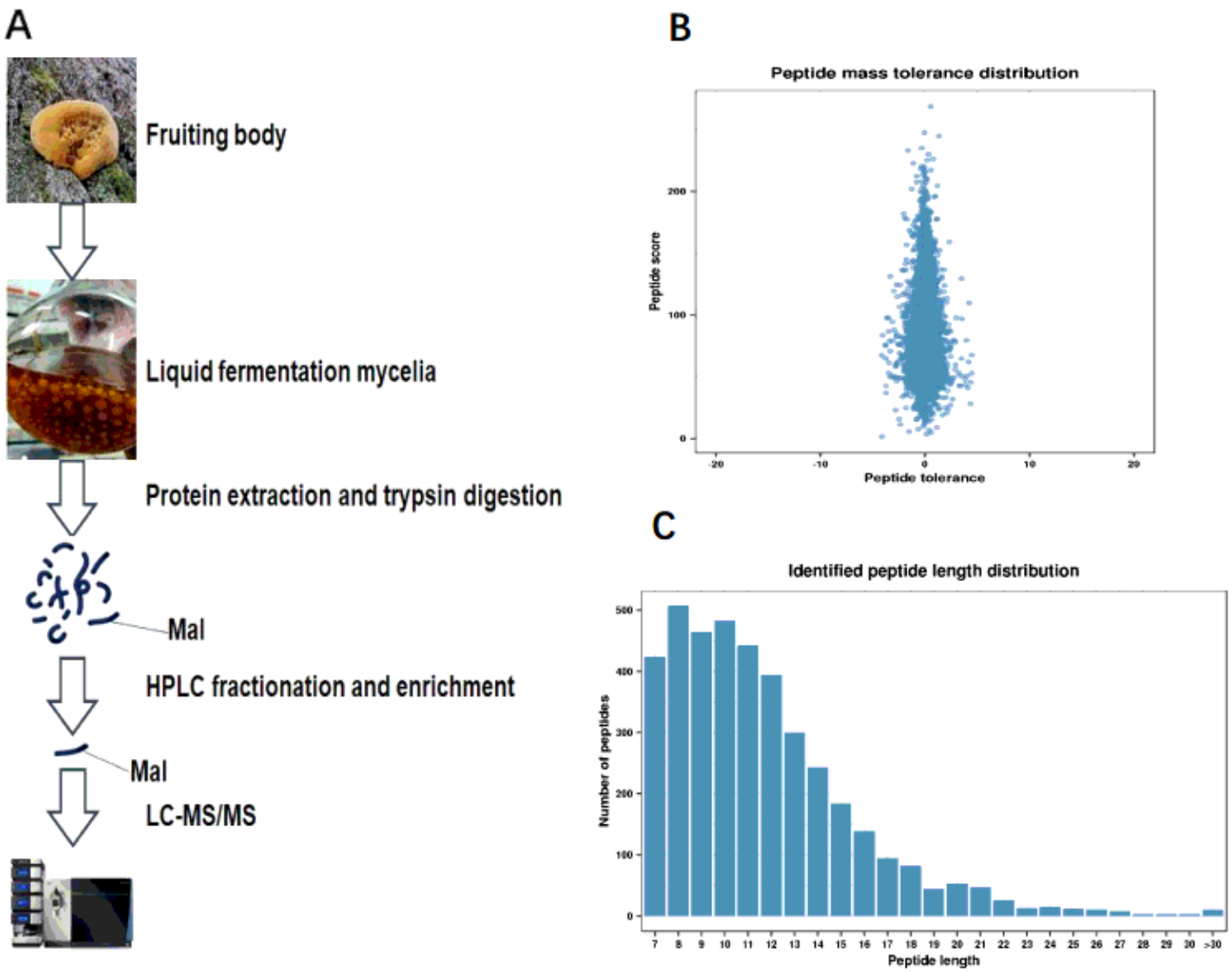

Figure 1

Analysis of malonylated sites in S. sanghuang. a Technology roadmap in this study. b Mass distribution of error for all malonyl peptides c Length distribution of modified peptides

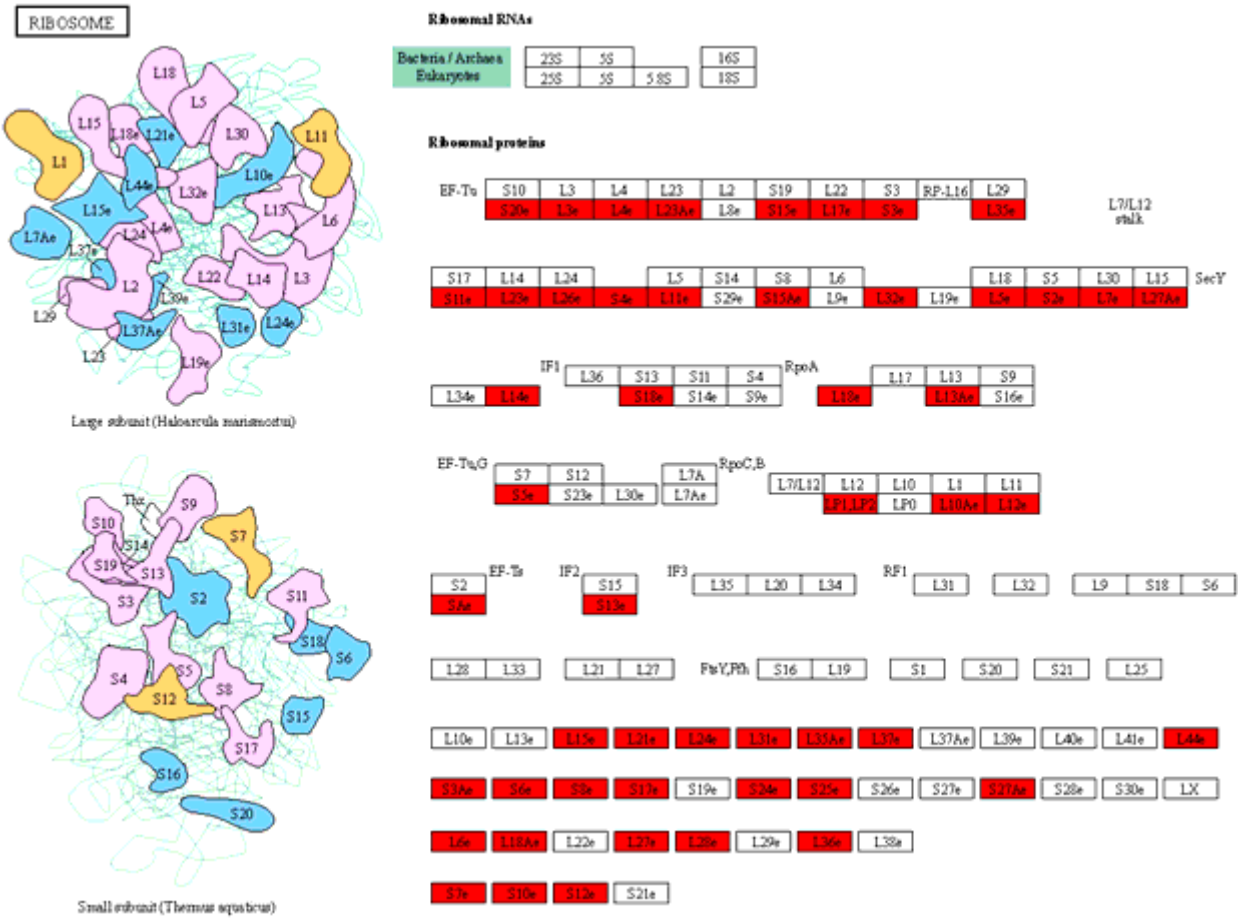

Figure 1

Malonylated modified sites on ribosomal proteins in S. sanghuang. The malonylated modified sites were highlighted in red.

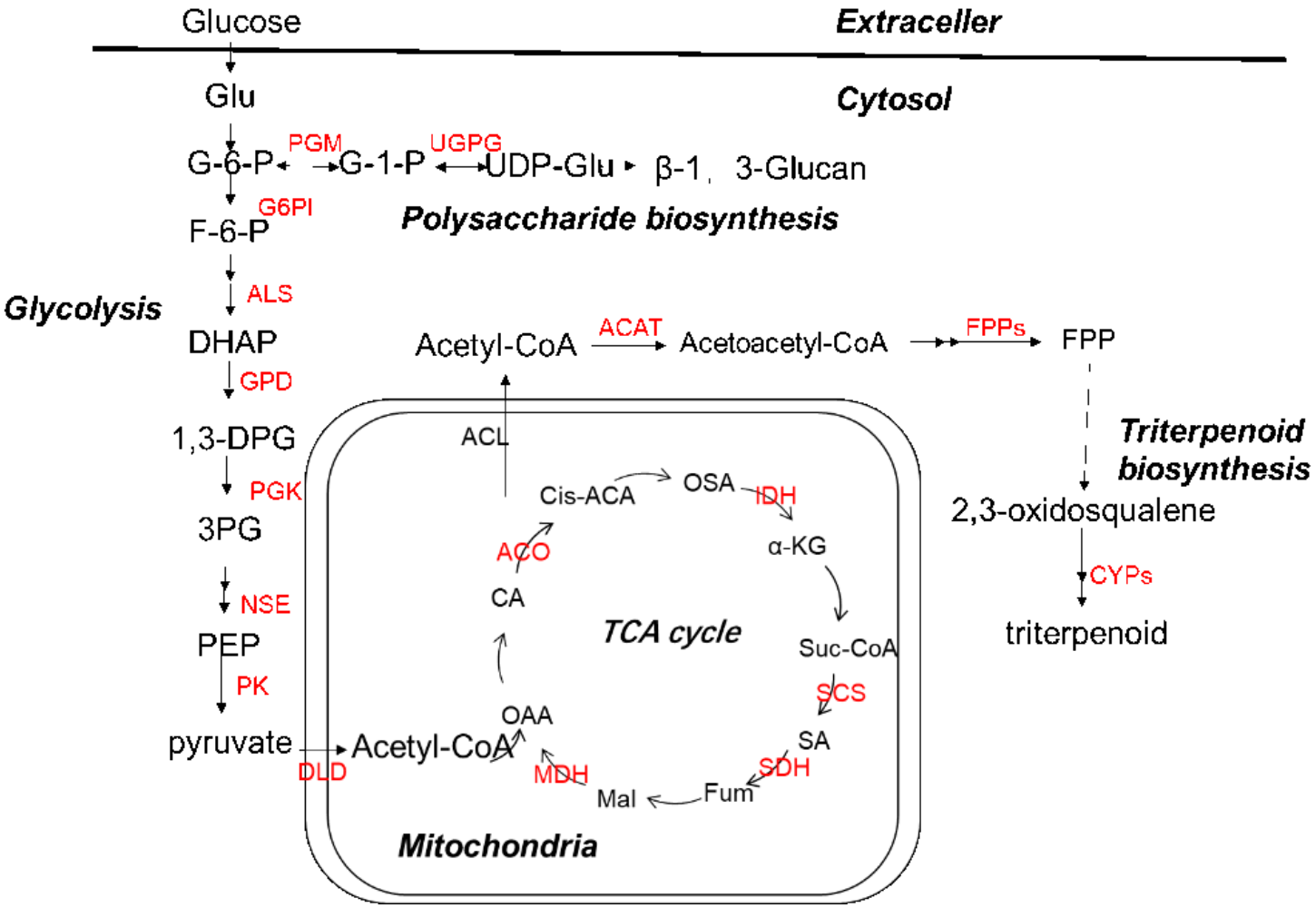

Figure 1

Biosynthesis of triterpenoid and polysaccharide in S. sanghuang. Malonylated proteins are highlighted in red. Additional file 2: Table S2 contains the enzyme annotation.

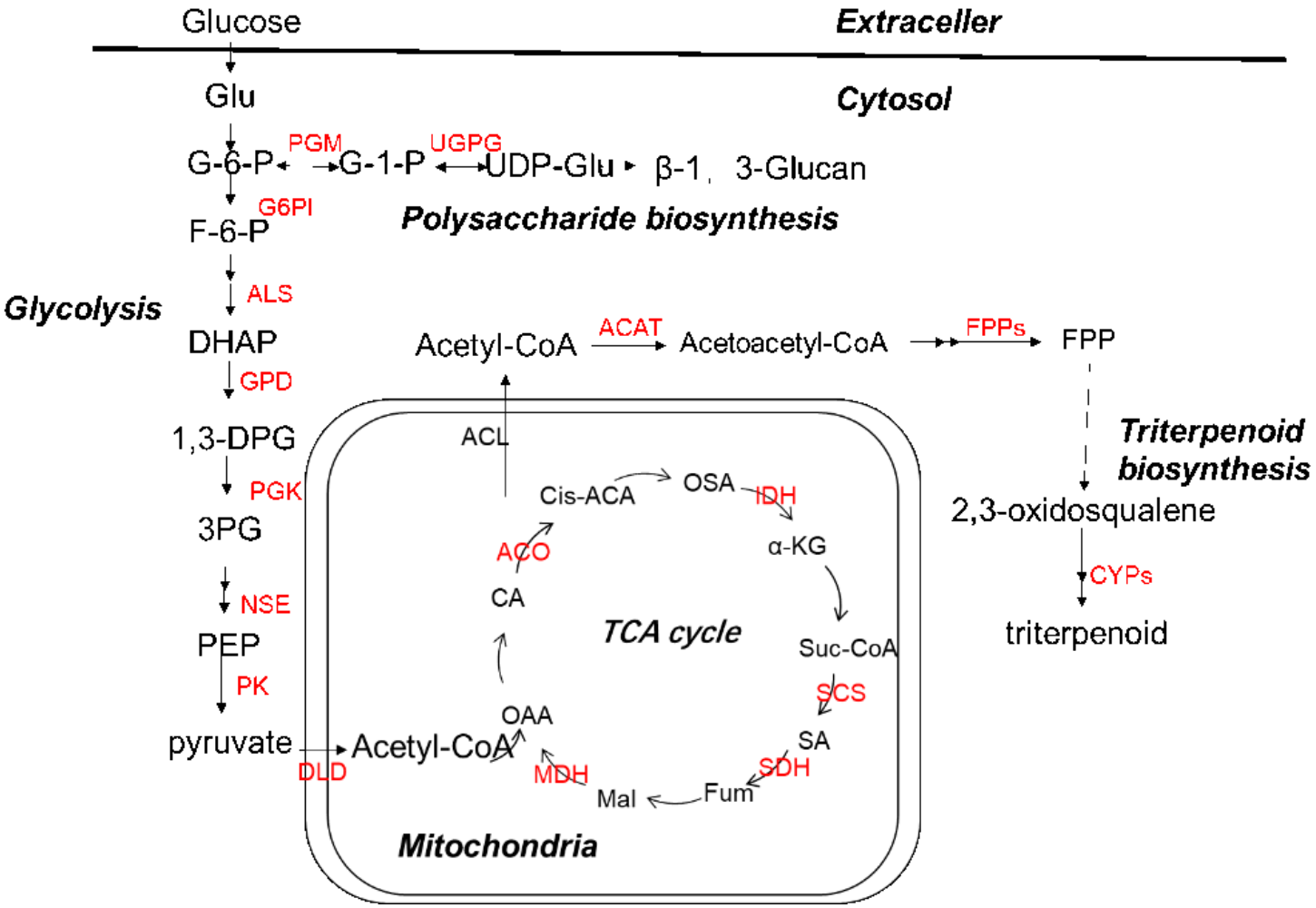

Figure 1

Biosynthesis of triterpenoid and polysaccharide in S. sanghuang. Malonylated proteins are highlighted in red. Additional file 2: Table S2 contains the enzyme annotation.

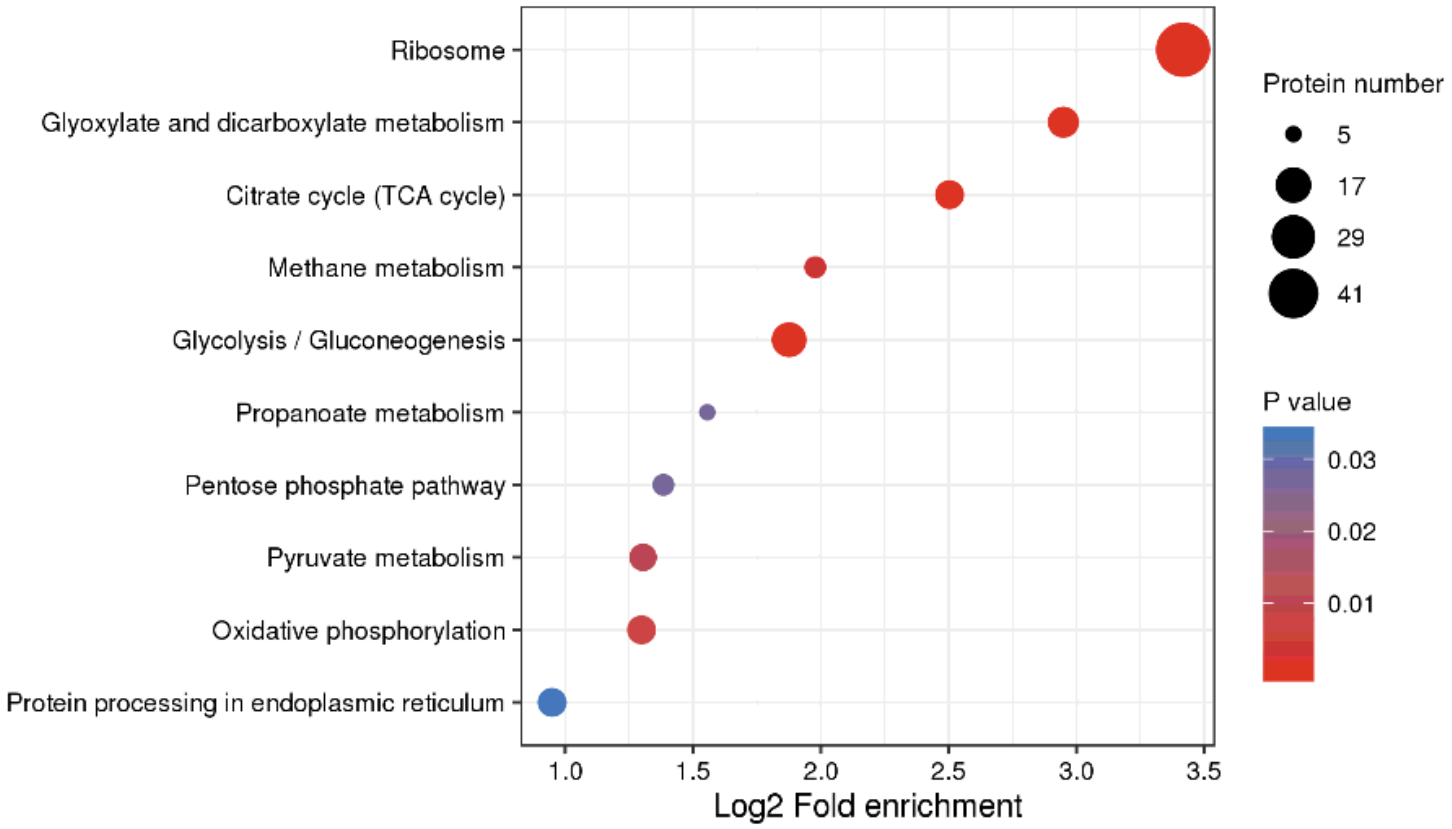

Figure 1

KEGG pathway enrichment bubble plot of proteins corresponding to modification sites in S. sanghuang

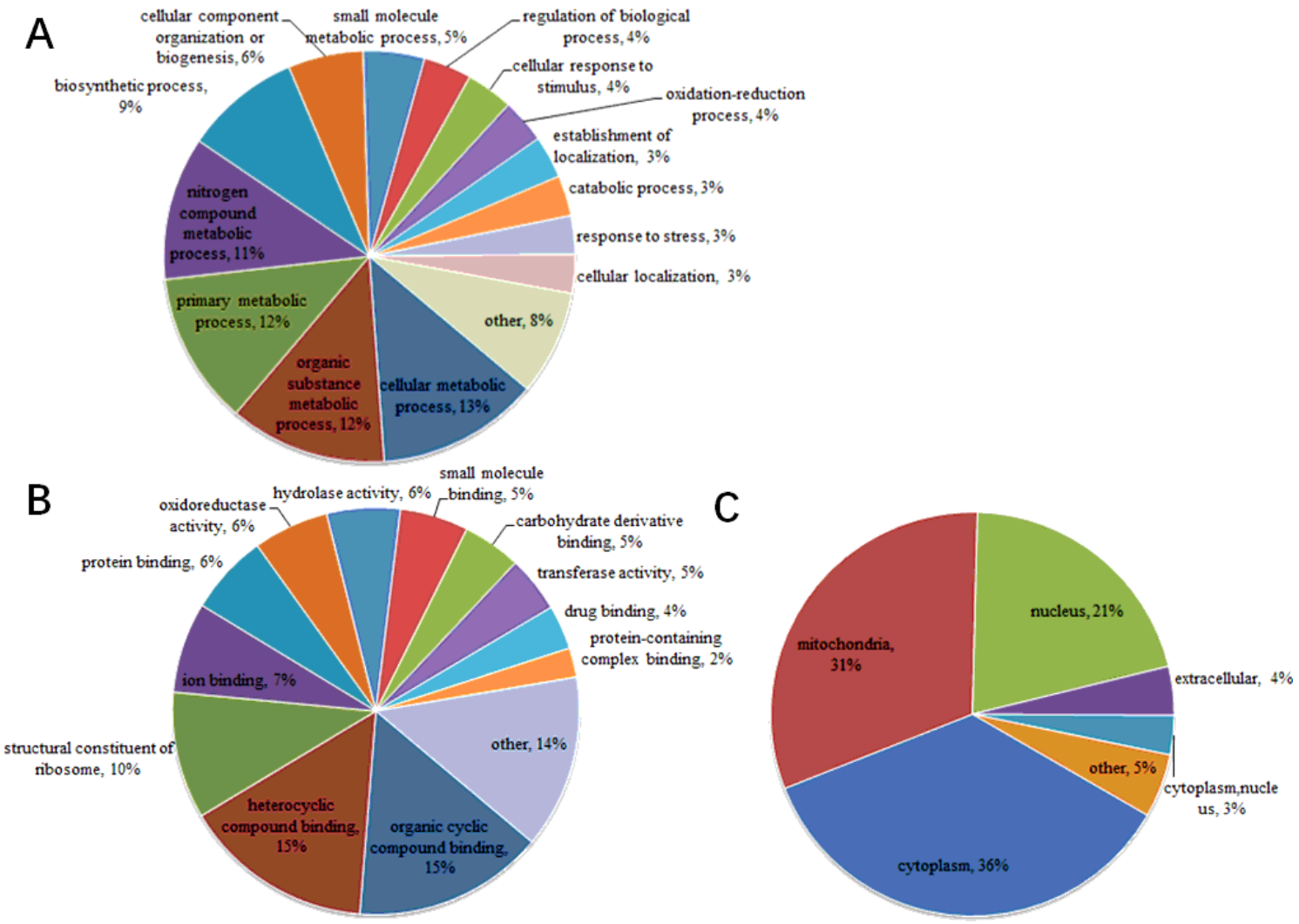

Figure 1

Functional classification of malonylated proteins in S. sanghuang. a Classify malonylated proteins based on biological process. b Classify malonylated proteins based on molecular function. c Subcellular localization of the malonylated proteins. The GO annotation classifies proteins according to their biological processes and molecular functions. A pie chart showing the percentage of malonylated proteins in each category.

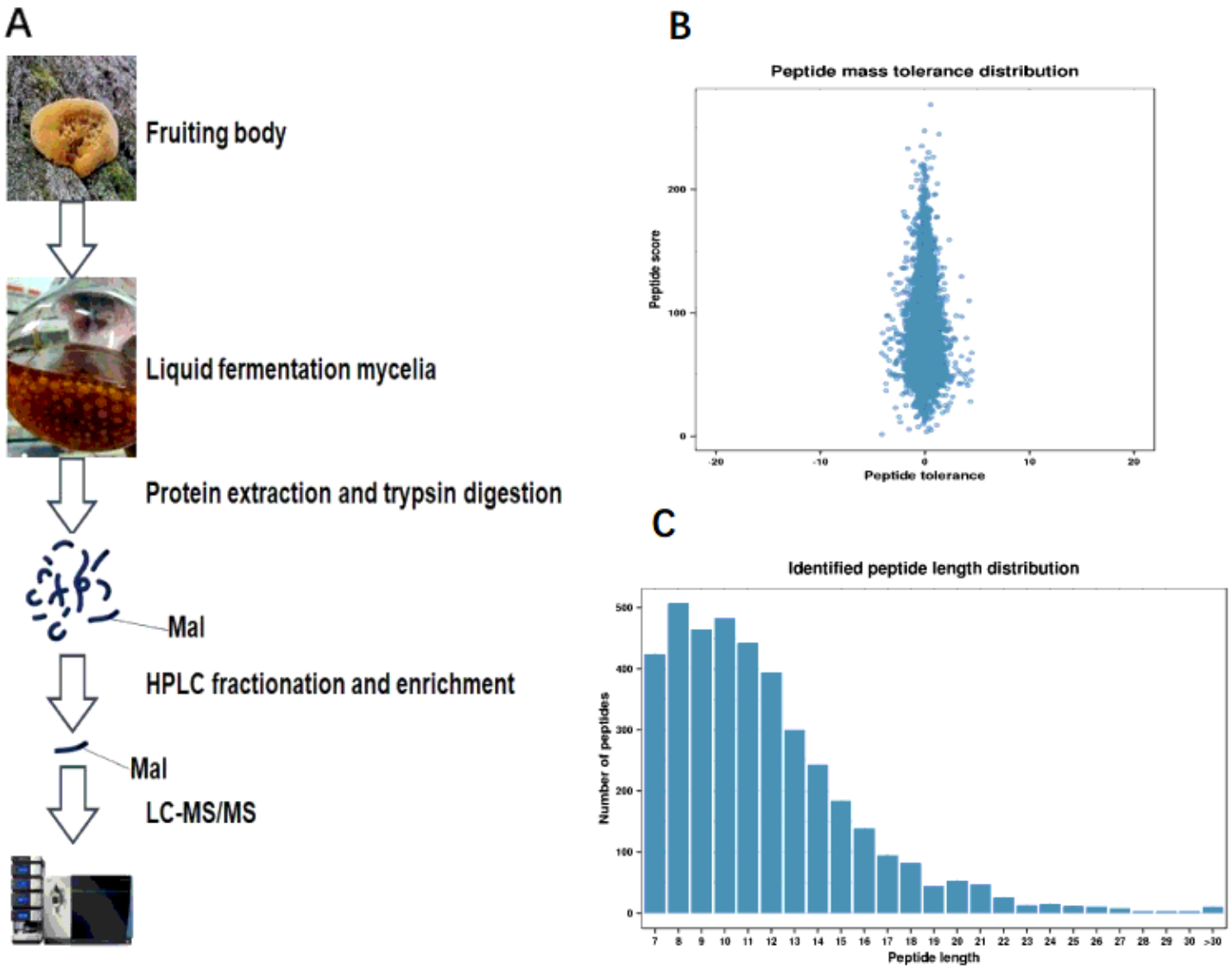

Figure 1

Analysis of malonylated sites in S. sanghuang. a Technology roadmap in this study. b Mass distribution of error for all malonyl peptides c Length distribution of modified peptides

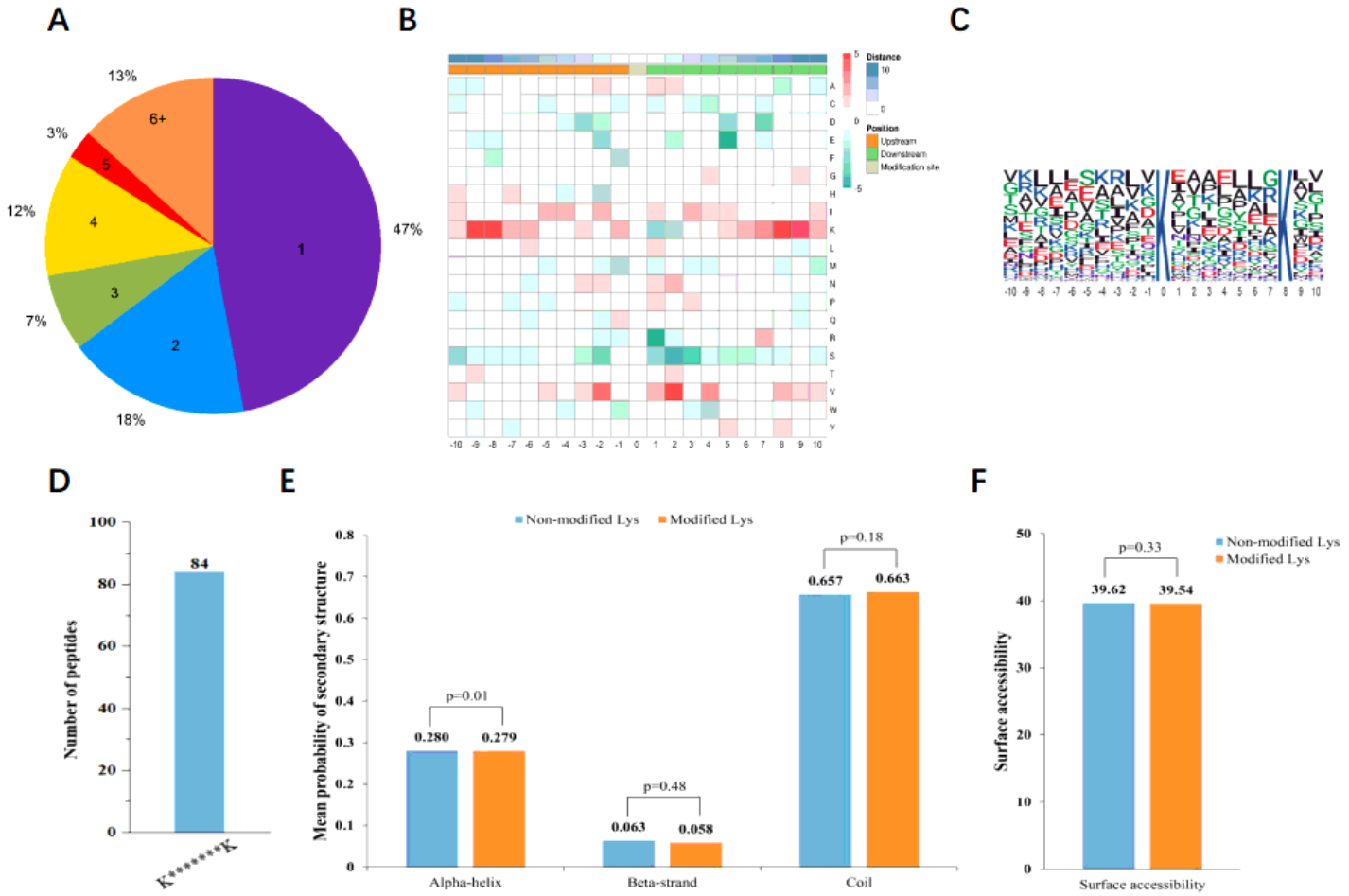

Figure 1

Characterization of malonylation sites. a Pie chart of the percentage and number of malonylated residues in the protein. b The frequency heat map of amino acid composition around malonylation c Conservatism of malonylation sites. Each letter's size pairs with the frequency of the amino acid at that site.. d Number of malonylation motif peptides. e Secondary structure analysis of malonyl protein. f Peptides surface accessibility of malonylation sites

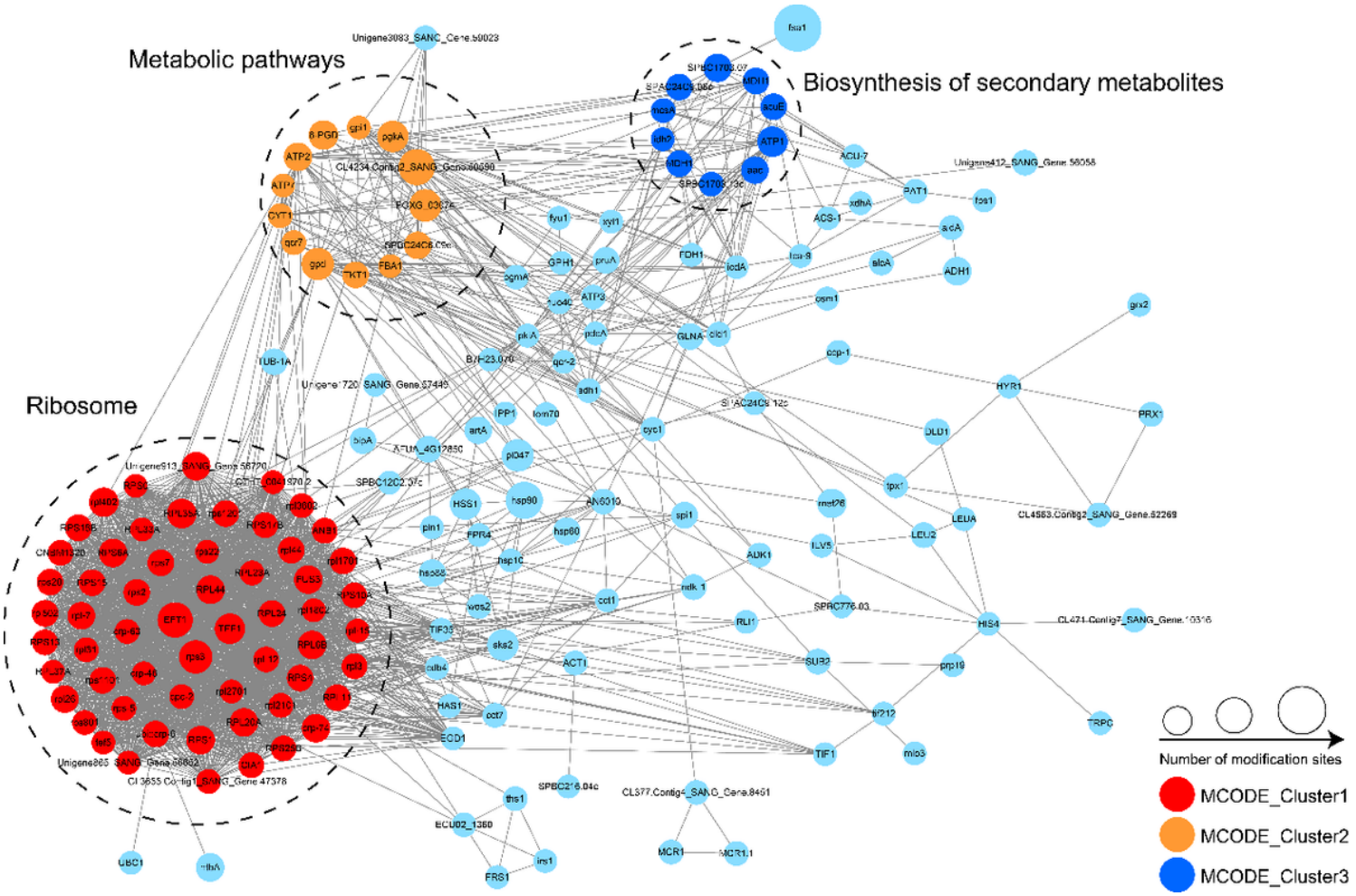

Figure 5

PPI network of malonylated proteins in S. sanghuang

Supplementary Files

This is a list of supplementary files associated with this preprint. Click to download.

- AdditionalFiles2TableS3.xlsx
- AdditionalFiles1FigureS1.docx
- AdditionalFiles1FigureS2.docx
- AdditionalFiles2TableS4.xlsx
- AdditionalFiles2TableS7.xlsx
- AdditionalFiles2TableS4.xlsx
- AdditionalFiles1FigureS2.docx
- AdditionalFiles1FigureS1.docx
- AdditionalFiles2TableS6.xlsx

- AdditionalFiles2TableS7.xlsx
- AdditionalFiles2TableS5.xlsx
- AdditionalFiles2TableS1.xlsx
- AdditionalFiles1FigureS3.docx
- AdditionalFiles1FigureS3.docx
- AdditionalFiles2TableS2.xlsx
- AdditionalFiles2TableS1.xlsx
- AdditionalFiles2TableS8.xlsx
- AdditionalFiles2TableS8.xlsx
- AdditionalFiles2TableS2.xlsx
- AdditionalFiles2TableS3.xlsx
- AdditionalFiles2TableS5.xlsx
- AdditionalFiles2TableS6.xlsx